AIP | Review of Scientific Instruments

High-intensity coherent vacuum ultraviolet source using unfocussed commercial dye lasers

Daniel R. Albert, David L. Proctor, and H. Floyd Davis

Citation: Rev. Sci. Instrum. **84**, 063104 (2013); doi: 10.1063/1.4806801
View online: http://dx.doi.org/10.1063/1.4806801
View Table of Contents: http://rsi.aip.org/resource/1/RSINAK/v84/i6
Published by the American Institute of Physics.

High-intensity coherent vacuum ultraviolet source using unfocussed commercial dye lasers

Daniel R. Albert, David L. Proctor, and H. Floyd Davis[a)]
Baker Laboratory, Department of Chemistry and Chemical Biology, Cornell University, Ithaca, New York 14853, USA

(Received 27 March 2013; accepted 2 May 2013; published online 11 June 2013)

Using two or three commercial pulsed nanosecond dye lasers pumped by a single 30 Hz Nd:YAG laser, generation of 0.10 mJ pulses at 125 nm (6×10^{13} photons/pulse) has been demonstrated by resonance enhanced four-wave mixing of collimated (unfocussed) laser beams in mercury (Hg) vapor. Phase matching at various vacuum ultraviolet (VUV) wavelengths is achieved by tuning one laser in the vicinity of the $6\ ^1S_0 \rightarrow 6\ ^3P_1$ resonance near 253.1 nm. A number of different mixing schemes are characterized. Our observations using broadband lasers ($\sim$0.15 cm^{-1} bandwidths) are compared to previous calculations pertaining to four-wave mixing of low intensity narrowband laser beams. Prospects for further increases in pulse energies are discussed. We find that VUV tuning curves and intensities are in good agreement with theoretical predictions. The utility of the VUV light source is demonstrated by "soft universal" single-photon VUV ionization in crossed molecular beam studies and for generation of light at 130.2 nm for oxygen atom Rydberg time-of-flight experiments. © *2013 AIP Publishing LLC*. [http://dx.doi.org/10.1063/1.4806801]

I. INTRODUCTION

Coherent radiation in the visible, infrared, and near ultraviolet can be readily produced using commercial lasers employing nonlinear frequency conversion in solid crystals.[1] However, since birefringent crystals are not capable of transmitting wavelengths shorter than $\sim$190 nm, coherent light sources in the vacuum ultraviolet (VUV) and extreme ultraviolet (XUV) employ gases rather than solids for nonlinear frequency conversion. Unfortunately, due to the low densities and small nonlinear susceptibilities of gases, conversion efficiencies producing $\lambda < 190$ nm are typically much less than 1%.[2–5]

In recent years, a number of alternative VUV and XUV light sources have been developed, including discharge lamps[6,7] and laser induced plasma sources.[8] However, these approaches are not generally applicable if high peak powers, high spectral purity, and high spatial coherence are required. The undulator beamline at Berkeley's Advanced Light Source, a third generation synchrotron,[9] provides $\sim 10^{16}$ photons/s with an energy resolution, $\Delta E/E$, of $\sim$1%.[9] However, the need for a dedicated facility limits applicability of this method to only a few sites worldwide.[9,10] Furthermore, the quasi-continuous nature of synchrotron radiation generally prohibits applications requiring high peak VUV or XUV powers such as materials processing or multiphoton spectroscopy. Also, many experiments can benefit greatly from the use of pulsed rather than continuous VUV light sources. Therefore, considerable effort has been devoted to increasing the efficiencies for nonlinear frequency conversion of tabletop pulsed lasers into the VUV and XUV region.

The earliest reports of nonlinear frequency conversion in gases involved third harmonic generation.[11,12] For example, the spectroscopically important Lyman-α at $\lambda = 121.6$ nm is readily produced by focusing the 364.8 nm output from a single commercial dye laser (typically operating at 10–30 Hz) into a gas cell containing Kr.[13] For input pulse energies of $\sim$10 mJ ($\tau \sim$ 6–20 ns), $\sim 10^{10}$ photons/pulse can be obtained in the VUV ($\nu_{VUV} = 3\nu_1$) corresponding to a conversion efficiency of $\sim 10^{-6}$. Other mixing schemes employing Kr or Xe using a single dye laser have been described, providing continuously tunable radiation between 110 and 210 nm.[2,14]

By using two input laser beams, one tuned to a two-photon atomic resonance, the resonance enhancement of χ^3 leads to substantially improved conversion efficiencies. For example, broadly tunable radiation near 10 eV can be generated by four-wave difference frequency mixing ($\nu_{VUV} = 2\nu_1 - \nu_2$) of focused lasers in Kr, producing $\sim 10^{11}$ photons/pulse.[15] For specific VUV wavelengths, phase matching (e.g., by addition of Ar) makes it possible to employ higher gas pressures, facilitating production of $\sim 10^{12}$ photons/pulse reported at Lyman-α using $\lambda_1 = 212.55$ nm and $\lambda_2 = 850$ nm.[3,16] However, for generation of high VUV intensities using difference frequency mixing of focused lasers, two major practical limitations are difficult to overcome: (1) it is difficult to generate input pulse energies at λ_1 (typically <220 nm) exceeding 1–2 mJ, and (2) the onset of dielectric breakdown using focused lasers generally limits maximum input pulse energies.

In general, for generation of high VUV pulse energies above 9.5 eV, a significant advantage to resonance enhanced sum frequency ($\nu_{VUV} = 2\nu_1 + \nu_2$) mixing over difference frequency ($\nu_{VUV} = 2\nu_1 - \nu_2$) mixing is that longer input wavelengths can be employed, allowing substantially higher input pulse energies. Sum frequency mixing schemes usually exhibit considerable variation in VUV conversion efficiencies with ν_2.[15] However, for many VUV applications, broad

a)Author to whom correspondence should be addressed: hfd1@cornell.edu

tunability is not necessary, and the primary goal is instead to achieve the highest possible VUV pulse energies at specific wavelengths, e.g., 130.2 nm for O atom detection, or ~125 nm for single photon ionization of organic radicals from bimolecular reactions. The application of VUV for ultrasensitive photoionization detection in analytical mass spectrometry has been discussed in some detail.[17]

While phase matching by the addition of gases such as Kr or Xe may be employed to enhance conversion efficiencies at certain wavelengths,[3,13,14] this is not always possible. For example, the efficiency for difference frequency mixing in Kr to generate 130.2 nm light needed for excitation of the $^3P_J \rightarrow {}^3S_1$ transition in oxygen atoms cannot be enhanced by adding Ar or Xe.[3] However, as discussed in detail below, by tuning *three* input laser beams in the vicinity of atomic resonances, phase matching can be achieved in the absence of additional gases, leading to great enhancement of VUV intensities.

Because of their very large χ^3, metallic vapors such as magnesium (Mg) and mercury (Hg) are frequently used to obtain substantially higher conversion efficiencies into the VUV and XUV.[18–22] For example, by focusing two lasers into Hg vapor, Hilbig and Wallenstein demonstrated that by tuning one laser to the $6\ {}^1S_0 \rightarrow 7\ {}^1S_0$ two-photon resonance at $\lambda_1 = 312.85$ nm,[19] up to ~0.5% conversion efficiency employing a second laser tunable in the visible region can be achieved, with the greatest efficiencies reported in the 125 nm (9.9 eV) range. In this way up to 10^{13} photons/pulse at a specific wavelength near 125 nm was reported.[19] Although theory predicts that for focused geometries in Hg using the $7\ {}^1S_0$ two-photon resonance, VUV generation should be limited to the high energy side of $^1P_1$ resonances below the Hg^+ limit (10.4 eV), in practice tunable light is also observed on the low energy side.[19] Thus the VUV conversion efficiency exhibits pronounced maxima near $^1P_1$ resonances. Although slightly less efficient, the 625.70 nm and 312.85 nm outputs from a *single* frequency-doubled dye laser can be used to produce very high VUV intensities at a single wavelength near 125 nm.[19]

All of the methods described above employ *focused* configurations for VUV generation. Usually, saturation and dielectric breakdown effects become significant as laser powers are increased, making it impossible to scale systems to higher pulse energies.[20] To avoid this limitation, Smith and Alford proposed a four-wave mixing scheme employing three unfocused tunable lasers for VUV generation in Hg vapor, as shown in Figure 1.[20] By tuning λ_1 near the 253 nm $6\ {}^1S_0 \rightarrow 3\ {}^3P_1$ resonance, λ_2 near 404 nm (corresponding to the $6\ {}^1S_0 \rightarrow 7\ {}^1S_0$ two-photon resonance), and λ_3 near 777 nm (near a $9\ {}^1P_1$ resonance), phase matching can be achieved while at the same time χ^3 is maximized due to the triply-resonant nature of the four-wave mixing process.[20] An attractive feature of this approach is that the system should be scalable to higher VUV pulse energies by using higher input pulse energies because of the use of collimated (unfocussed) lasers. Using this method, Muller *et al.* produced ~1.2 mJ/pulse (8×10^{14} photons/pulse) at 130.2 nm, corresponding to the $^3P_2 \rightarrow {}^3S_1$ transition in oxygen atoms.[21] In their work, the 8 mm diameter input beams, each around 10 mJ/pulse, ($\tau = 2.2$ ns)

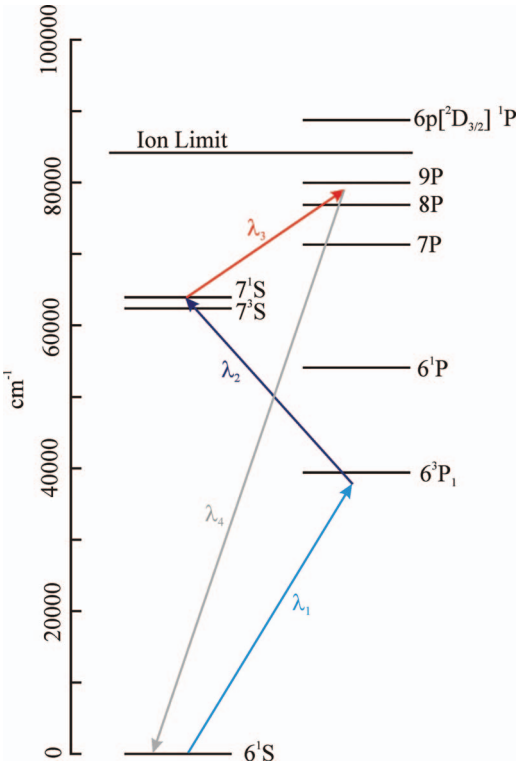

FIG. 1. Energy level diagram of selected states of mercury. λ_1 is tuned near a single photon resonance ($6\ {}^1S_0 \rightarrow 6\ {}^3P_1$), λ_2 is tuned so that $\lambda_1 + \lambda_2$ is two-photon resonant ($6\ {}^1S_0 \rightarrow 7\ {}^1S_0$) and λ_3 is tuned near a Rydberg resonance ($9\ {}^1P_1$). The resulting sum frequency is generated at $\lambda_4 \approx 125$ nm.

were of single longitudinal mode (SLM) with near- transform-limited bandwidths. Their system was extremely complex, employing three separate ring dye laser oscillators followed by dye and titanium sapphire amplifiers pumped by Nd:YAG lasers.[21] Since that time, no further work has been reported for pulsed VUV using this method. However, several groups have employed this triply-resonant scheme using three tunable continuous-wave lasers in focused configurations in Hg for producing continuous-wave VUV radiation at unprecedented intensities.[23,24]

On the basis of the previous theoretical and experimental work, it was not at all obvious that the remarkably high VUV intensities reported by Muller *et al.*[21] might be achieved by four wave mixing of *unfocussed* commercial multimode dye lasers. However, using output beams from commercial lasers with a Hg oven in an arrangement similar to that of Hilbig and Wallenstein[19] in our laboratory, we found that substantial VUV intensities near 9.9 eV could be produced in a 2 cm long Hg cell *with the focusing lens removed*. Subsequently, by employing substantially longer Hg heat pipes, we have optimized conditions for producing very high VUV intensities by mixing through the $7\ {}^1S_0$ state in mercury using unfocussed configurations. We have used these VUV beams for "soft" single photon VUV ionization in crossed molecular beam scattering experiments[25] as well as at 130.2 nm for oxygen atom Rydberg time-of-flight (ORTOF) spectroscopy studies.[26]

In our laboratory over the past few years, a number of different schemes have been employed for VUV generation using two or three commercial dye lasers and, in some cases, the 266.1 nm radiation (fourth harmonic) of the injection-

seeded Nd:YAG laser. Here we present intensity measurements and tuning curves for generating radiation near 125 nm, and demonstrate the light source for 130.2 nm radiation in ORTOF studies. We provide a detailed description of a design that easily eliminates laser damage of windows due to contamination issues, a common problem using mercury as the nonlinear material. An off-axis MgF_2 lens is used to separate the VUV from the residual visible and UV beams. Comparisons are made to the detailed calculations by Smith and Alford.[20]

II. EXPERIMENTAL

The VUV radiation was generated by resonance-enhanced four-wave mixing in mercury vapor.[20] The tunable input beams were generated using two or three commercial pulsed dye lasers (Scanmate 2) pumped by a single injection-seeded Nd:YAG laser (Continuum Powerlite 9030 or Precision 9030). The dye lasers were pumped at either 532 nm or 355 nm, corresponding to the second and third harmonics of the Nd:YAG laser, respectively. The dye laser beams were typically ∼2 mm diameter. In some cases the fourth harmonic (266.1 nm) of the Nd:YAG pump laser was telescoped to ∼2 mm diameter and used as λ_1 in the four wave mixing scheme. In all cases, the optical pathlengths for λ_1, λ_2, and λ_3 were matched (to within about 2 cm) to ensure that all three pulses were temporally overlapped in the heat pipe. The polarizations of all three lasers were linear, with λ_1 and λ_2 parallel. The output VUV polarization is parallel to λ_3.

The three laser beams were propagated separately via dielectric mirrors and then combined on a fused silica Pellin-Broka prism located near the entrance to the heat pipe. The use of a Pellin-Broka prism in a "reverse geometry" (i.e., to combine beams of different wavelengths) provides two significant advantages: (1) three separate wavelengths can be easily combined without the need for expensive dichroic mirrors, and (2) by using the prism with P-polarization for all three laser beams, reflective losses are negligible. The input window to the heat pipe was mounted at Brewster's angle to further minimize reflective losses.

The heat pipe consisted of 2.5 cm outside diameter (OD) stainless steel tubing with 20 cm of water cooling (∼ 293 K) on each end of the tube (Figure 2). To assemble the heat pipe, thermocouples were first attached to the stainless steel tube in five locations in order to monitor the temperature. The center 60 cm of the tube was then wrapped with several layers of

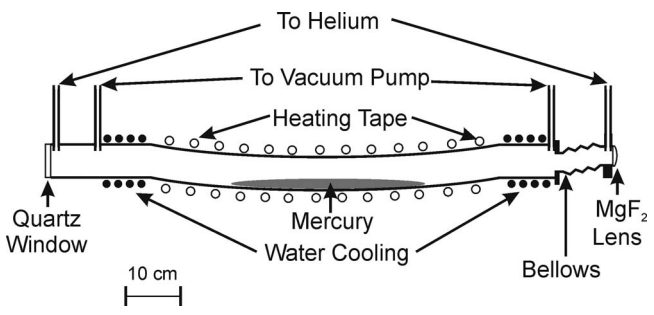

FIG. 2. Schematic of the mercury heat pipe.

0.050 in. thick copper sheet followed by three heating tapes surrounded by several layers of aluminum foil. The central portion of the tube (60 cm) was heated to ∼410 K generating ∼1 Torr of Hg vapor. A pool of mercury was held in the center of the tube by a slight bend on both sides of the tube so that the mercury pool was held in the center 60 cm of the tube. Liquid mercury condensed in the water-cooled region of the tube returns to the lowest central region due to gravity. The tube was evacuated using a dual stage rotary pump and a slow flow of helium (∼10 Torr) was directed away from each end of the tube to keep the optics clean. The helium entered at each end of the cell, approximately 3 cm from the window surface, and exited at each end of the cell ∼10 cm from the windows. The helium flow rate was controlled by needle valves on both the inlet and outlet. The flow is sufficiently slow that a cylinder of helium lasts for several months of continuous flow.

The energy level diagram for atomic mercury is shown in Fig. 1. The first photon (λ_1) near 255 nm was typically generated by frequency doubling the 765 nm light from the output of a 532 nm pumped dye laser (LDS 765 laser dye) and then mixing the doubled light with the residual 765 nm radiation. Since a 382.5 nm waveplate was not available, a 266 nm waveplate was used between the doubling crystal and the mixing crystal in order to rotate the polarization of the 382.5 nm light to achieve optimal mixing. The waveplate was angle tuned to maximize the 255 nm light intensity. In some experiments, the 255 nm light was produced by frequency doubling the 510 nm output from a 355 nm pumped dye laser. Typical pulse energies used in these experiments were 2–3 mJ/pulse at 255 nm. The second photon (λ_2) near 404 nm was generated either by pumping a mixture of Exalite 404 (Exciton) in dioxane at 355 nm or by mixing the ∼651 nm light from a 532 nm pumped dye laser (DCM or Pyridine 1 laser dye) with the 1064 nm light from the injection seeded Nd:YAG laser. Typical pulse energies at 404 nm were 6–10 mJ/pulse. The third photon (λ_3) near 630 nm or 777 nm was generated directly from a 532 nm pumped dye laser (DCM or LDS 765 laser dye, respectively). Typical pulse energies at 630 nm or 777 nm were 7–8 mJ/pulse.

We have also generated VUV pulses using only two dye lasers. For example, using $\lambda_1 = \lambda_2 = 312.76$ nm (10 mJ/pulse) and $\lambda_3 = 630$ nm, light near 9.9 eV is generated. Alternatively, $\lambda_1 = 266.1$ nm, obtained as the fourth harmonic of an injection seeded Nd:YAG laser with the two-photon resonance achieved using $\lambda_2 = 379.5$ nm, generated by mixing 589 nm light (Kiton Red laser dye) with 1064 nm fundamental from the Nd:YAG laser. Typical pulse energies were 10 mJ at both 266.1 nm and 379.5 nm. While much higher 266.1 nm pulse energies were achievable, after telescoping to ∼2 mm diameter, mirror damage occurred at pulse energies above 10 mJ.

In order to isolate the VUV beam from the three strong residual UV and visible beams, they are dispersed by a 50 cm focal length MgF_2 lens (2.54 cm diameter) by propagating the beams off of the optic axis of the lens. The MgF_2 lens also served as the output window of the mercury cell. The lens was mounted in an o-ring sealed homemade lens mount machined from a 2.75 in. OD double-sided conflat flange. The lens mount was connected to the mercury cell using a commercial

4 in. long bellows with 2.75 in. conflat flanges at both ends, as illustrated in Figure 2. The lens mount was rigidly supported on a one-dimensional translation stage and a second 4 in. long bellows assembly connected the lens to the apparatus. This arrangement made it possible to translate the lens horizontally while the mercury cell and vacuum system remained stationary.

For initial alignment of the lasers and MgF_2 lens, a red helium neon laser was counter propagated through the photoionization region, edge of the MgF_2 lens, VUV cell, and Pellin-Broka prism towards the three dye lasers. The λ_3 laser was then overlapped with the red helium neon laser and then the alignment of lasers at λ_1 and λ_2 adjusted to achieve good spatial overlap. Due to the much larger index of refraction for the VUV beam, the final position of the MgF_2 lens must be adjusted using the translation stage to precisely locate the VUV beam at the ionization region of the detector. After all beams are aligned and the VUV intensity optimized and spatially aligned, the macor beam dump, held on a vacuum compatible linear manipulator was then translated horizontally to block the 255, 404, and 630 nm beams while allowing the 125 nm light to pass.

The high intensity VUV light source at 125 nm was coupled to the Cornell rotatable source, fixed-detector crossed molecular beams apparatus for "soft" single photon ionization.[25,27] The high intensity light source at 130.2 nm was used on a different apparatus, employing a fixed source and rotatable detector, for studies involving ORTOF.[26] In ORTOF, another tunable laser near 305 nm is used to excite oxygen atoms from the 3 $^3S_1$ state to a high lying long-lived Rydberg state.[26] The Rydberg atoms drifted ~33.3 cm before being passing through a grounded mesh and being field ionized and detected using a microchannel plate detector.

In the rotatable source machine, no additional optical elements were present between the MgF_2 dispersing lens and the ionization region of a quadrupole mass spectrometer where the base pressure was $<1 \times 10^{-10}$ Torr. An isolation valve and two stages of differential pumping (employing two turbomolecular pumps) were used. In the Rydberg machine, after the residual beams were dumped, the VUV was reflected into the apparatus using a protected aluminum mirror (E-source optics) mounted in a 5-way 8 in. conflat cross pumped by a turbomolecular pump.

All of the intensity measurements were recorded using the rotatable source, fixed detector apparatus by monitoring the wide angle inelastic scattering of chlorobenzene (C_6H_5Cl) off of molecular oxygen (O_2). The C_6H_5Cl beam was produced by bubbling H_2 carrier gas (20 psi (gauge)) through a room-temperature liquid C_6H_5Cl sample and expanding the mixture through the 1 mm orifice of a piezoelectrically actuated pulsed valve.[28,29] The molecular beam was skimmed by a 2 mm diameter skimmer before entering the main chamber and crossing the O_2 beam. The O_2 beam was produced by expanding a 40% O_2 in He mixture (40 psi (gauge)) through the 1 mm orifice of a second piezoelectrically actuated pulsed valve. The beam was skimmed by 1.5 mm diameter skimmer before entering the main chamber and crossing the C_6H_5Cl beam. After the beams cross, the non-reactively scattered components are monitored at various lab angles (15°–30°). The scattered components travel ~25 cm before they are ionized by the 125 nm VUV beam. The ions are then mass filtered using a quadrupole mass analyzer (Extrel) and counted using an electron multiplier/conversion dynode set-up. For comparison measurements between a 7.9 eV excimer laser (GAM EX-100HF) and our 125 nm light source the nonreactive scattering of n-methylaniline was monitored since it can be ionized at both 7.9 and 9.9 eV.

III. REVIEW OF THEORETICAL CALCULATIONS

The calculations based on the measured refractive indices and nonlinear susceptibilities of Hg vapor, published by Smith and Alford in 1987,[20] are of great value for predicting tuning curves and nonlinear conversion efficiencies employing collimated (unfocussed) pulsed laser beams. Before discussing our experimental results, we briefly review some of their results.

Figure 3 shows the partial Δk, calculated by Smith and Alford, for mixing of collimated low-intensity lasers as a function of frequency near the $^3P_1$ Hg resonance at $\nu = 39\,412$ cm^{-1} ($\lambda = 253.7$ nm), and the 9p $^3P_1$ and $^1P_1$ resonances near 80 000 cm^{-1}.[20] For a given choice of ν_1, the value of Δk_1 in the vicinity of the $^3P_1$ resonance is first read directly from Fig. 3. For collimated laser beams, the VUV frequency where phase matching occurs, corresponding to the same partial Δk, is then read from Figure 3. For example, for $\lambda_1 = \lambda_2 = 312.85$ nm, corresponding to the two-photon resonance in Hg at 31 964 cm^{-1}, $\Delta k_1 = 0.18$ is indicated by the dotted horizontal line. As indicated in Fig. 3, the optimum VUV frequency (ν_{vuv}) corresponding to the same value of Δk lies approximately halfway between the $^3P_1$ and $^1P_1$ resonances, i.e., near $\nu_{vuv} = 79\,688$ cm^{-1}. Using the two-photon resonance frequency of 63 928 cm^{-1}, the optimum phase matching input wavelength, λ_3 is calculated to be 634.5 nm.

The partial susceptibilities χ_p, plotted in Fig. 4, can be used to estimate relative VUV intensities for various specific combinations of ν_1 and ν_{VUV}. As described by Smith

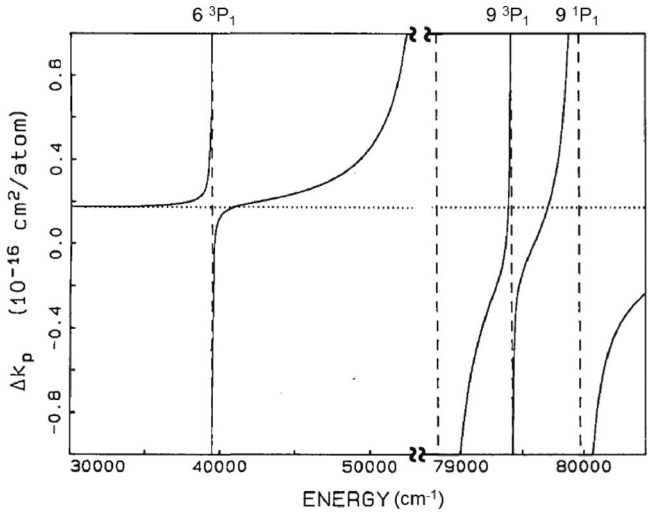

FIG. 3. Partial Δk as a function of frequency near the 6 $^3P_1$ and 9 $^3P_1$ and 9 $^1P_1$ resonances. Note change in horizontal axis and scale. Reprinted with permission from A. V. Smith and W. J. Alford, J. Opt. Soc. Am. B **4**, 1765 (1987). Copyright 1987 Optical Society of America.

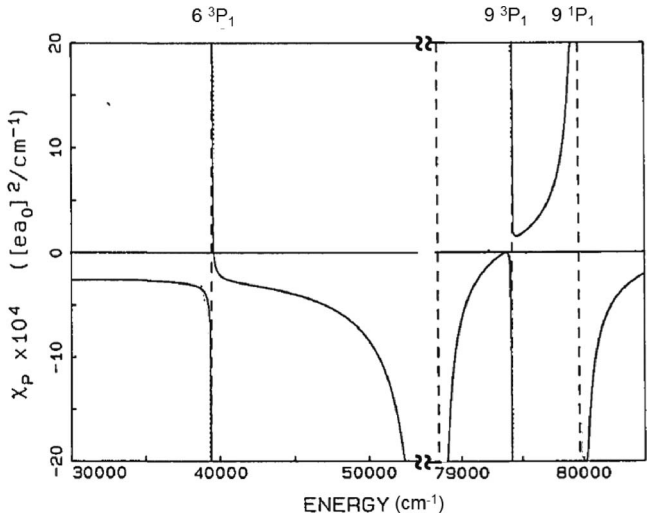

FIG. 4. Partial susceptibilities χ_P as a function of frequency near the 6 $^3P_1$ and 9 $^3P_1$ and 9 $^1P_1$ resonances. Solid lines are for the 7 $^1S_0$ resonance studied in this work. Note change in horizontal axis and scale. Reprinted with permission from A. V. Smith and W. J. Alford, J. Opt. Soc. Am. B **4**, 1765 (1987). Copyright 1987 Optical Society of America.

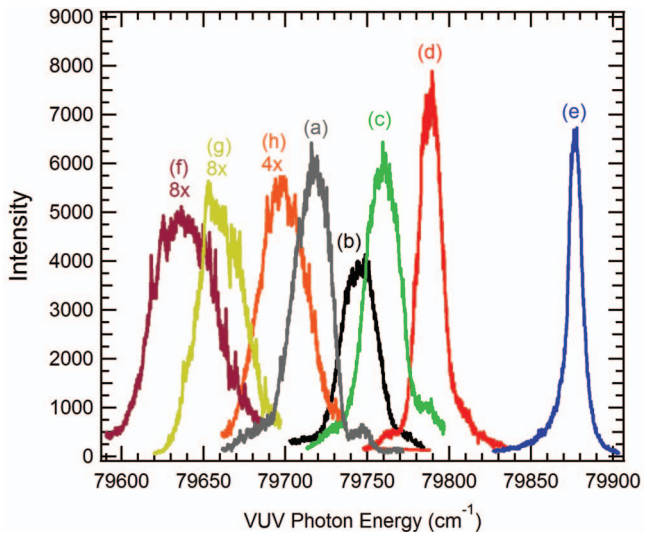

FIG. 5. Tuning curves for VUV generation (tuning λ_3) when $\lambda_1 + \lambda_2 = 63\,928$ cm^{-1} for the following λ_1 values with mJ/pulse of λ_1 in parenthesis. See Table I for corresponding values for λ_2. The 6 $^1S_0 \rightarrow 6\ ^3P_1$ resonance in mercury is at 253.7 nm (39 412 cm^{-1}). All curves are not scaled except for those marked in the figure (a) 266.1 nm (10 mJ), (b) 256.6 nm (1.3 mJ), (c) 255.7 nm (2.5 mJ), (d) 254.8 nm (2.7 mJ), (e) 254.0 nm (2.7 mJ), (f) 252.1 nm (1.5 mJ), (g) 251.6 nm (1.3 mJ), (h) 247.9 nm (1.5 mJ).

and Alford, the third order nonlinear susceptibility $\chi^{(3)}$ is proportional to the magnitude of the product $\chi_1 \times \chi_{VUV}$.[20] With ν_1 detuned to frequencies significantly lower than the $^3P_1$ resonance at 39 412 cm^{-1}, χ_1 is approximately constant at −2.5 and, under phase matching conditions with $\nu_{vuv} = 79\,688$ cm^{-1}, the corresponding $\chi_{VUV} \approx 2.5$. As described below, this scheme is attractive in terms of experimental simplicity because only two relatively efficient DCM dye lasers are required, operating at 312.85 nm and ∼634.5 nm.

Using three independently tunable lasers, one can tune ν_1 to higher frequencies on the low energy side of the $^3P_1$ resonance while simultaneously tuning ν_2 to remain on the 7 $^1S_0$ two-photon resonance (Fig. 1). Under these conditions, Fig. 3 indicates that ν_{VUV} shifts slightly to the blue and, according to Fig. 4, VUV intensities will increase slightly. However, as ν_1 is tuned very close to the $^3P_1$ resonance from the low energy side, Δk_1 increases sharply. To maintain phase matching conditions, ν_{vuv} shifts to higher frequency, requiring progressively greater ν_3 as the 9 $^1P_1$ resonance at $\nu = 79\,964$ cm^{-1} is approached. As indicated in Fig. 4, χ_1 and χ_{VUV} both increase sharply in the vicinity of atomic resonances, so the largest VUV conversion efficiencies are predicted for $\lambda_1 \approx 255$ nm, $\lambda_2 \approx 404$ nm, and $\lambda_3 \approx 628$ nm, producing VUV light at wavelengths near 125 nm ($\nu_{VUV} \approx 79\,850$ cm^{-1}).

With ν_1 tuned to frequencies greater than 39 412 cm^{-1}, i.e., on the high energy side of the $^3P_1$ resonance, qualitatively similar behavior is predicted. However, since Δk_1 is negative close to the 6 $^3P_1$ resonance, phase matching requires tuning of ν_3 so ν_{VUV} is on the blue side of the $^3P_1$ or $^1P_1$ resonances. It should be noted, however, that because χ_1 changes sign (goes through zero) at frequencies ν_1 just above 39 412 cm^{-1}, the VUV conversion efficiencies will exhibit a considerably more complex frequency dependence.

IV. RESULTS AND DISCUSSION

A. VUV generation near 125 nm

Relative intensity measurements for a number of resonant two-photon mixing schemes, all employing the 7 $^1S_0$ state at 63 928 cm^{-1}, are shown in Figure 5. Table I lists the wavelengths employed for the different VUV generation schemes studied in our laboratory. Each tuning curve shown in Figure 5 represents a different two-photon combination (λ_1 and λ_2) and shows the resulting λ_3 tuning curve. Tuning curve (a) was obtained with $\lambda_1 = 266.1$ nm (fourth harmonic of the Nd:YAG laser) and $\lambda_2 = 379.5$ nm. The tuning curve of λ_3 was recorded by scanning λ_3 while monitoring the nonreactive scattering of C_6H_5Cl from O_2. For this scheme, only two tunable lasers are required. As shown in Figs. 3 and 4, for significant detuning of ν_1 below the 6 $^3P_1$ resonance, Δk_1, χ_1, and χ_{VUV} are all approximately constant so conversion efficiencies do not vary significantly with ν_1 and ν_2. Because relatively high UV pulse energies (10 mJ for each

TABLE I. Wavelengths (nm) used for resonance enhanced four-wave mixing in Hg vapor.

λ_1	λ_2	λ_3	λ_4
266.1	379.5	633.6	125.45
256.6	400.7	632.0	125.39
255.7	402.9	631.4	125.37
254.8	405.2	630.2	125.32
254.0	407.2	627.0	125.20
252.1	412.2	636.5	125.57
251.6	413.5	635.9	125.54
247.9	423.9	634.0	125.47

laser) can be generated as the Nd:YAG fourth harmonic and at 379.5 nm (the latter by mixing the Nd:YAG fundamental with 590 nm light), and because only two dye lasers are required, this scheme has been used quite extensively in our laboratory.

Because the Nd:YAG laser is injection seeded by a narrowband cw diode laser, the bandwidth of the 266.1 nm laser is nearly Fourier transform limited with bandwidth of <0.005 cm^{-1}. Somewhat surprisingly, we found that the VUV intensity did not decrease significantly when the injection seeder was turned off with the Nd:YAG fundamental bandwidth increasing to $\sim$1 cm^{-1}. Consequently, the bandwidths of ν_1 and ν_2 increase from <0.010 cm^{-1} and 0.15 cm^{-1} to 2 cm^{-1} and 1 cm^{-1}, respectively. While we have not studied this behavior extensively, this observation suggests that VUV conversion efficiencies under our specific experimental conditions are not strongly dependent on input laser bandwidths.

On the basis of Fig. 3, it is not surprising that the VUV tuning curve employing the 2-photon 7 ^{1}S$_0$ resonance at $\lambda_1 = \lambda_2 = 312.85$ nm (not shown) was found to be very similar to that shown in Fig. 5(a). However, the absolute VUV intensities using the 312.85 nm two-photon resonance were about a factor of two smaller under our experimental conditions. Because of its relative simplicity, employing the two-photon resonance is the most convenient possible approach for generation of high-intensity VUV using collimated lasers. In our laboratory, typically 10 mJ pulses at 312.85 nm (30 Hz) could be produced routinely. At the expense of somewhat greater complexity (using two dye lasers + fourth harmonic of Nd:YAG), the scheme with $\lambda_1 = 266.1$ nm (10 mJ) and $\lambda_2 = 379.1$ nm (10 mJ), we typically obtained a factor of 2 higher VUV intensities. The higher intensity using 266.1 nm scheme is entirely attributable to the factor of 2 greater total laser pulse energies at λ_1 and λ_2. As shown in curves (b)–(d), upon tuning λ_1 closer to the 6 ^{3}P$_1$ resonance, a gradual increase in VUV intensity is observed. Note that curve (d) was obtained with 254.8 nm pulse energies around 2.7 mJ, whereas curve (a) employed 266.1 nm pulse energies around 10 mJ. Clearly, conversion efficiencies increase significantly (by a factor of 4) as the ν_1 approaches the 6 ^{3}P$_1$ resonance. It is interesting to note, however, that according to curve (e), obtained with $\lambda_1 = 254.0$ nm (only 38 cm^{-1} below the 6 ^{3}P$_1$ resonance), maximum VUV intensities do not further increase as the 6 ^{3}P$_1$ resonance is approached. Clearly, factors other than those indicated in Fig. 4 (e.g., absorption in the VUV by Hg_2) are operative, effectively limiting conversion efficiencies close to the 6 ^{3}P$_1$ resonance. Our limited studies of the effect of Hg vapor pressure (by changing the temperature) suggest that peak VUV conversion efficiencies remain approximately constant when ν_1 is tuned over a range of about 200 cm^{-1} on the low energy (red) side of the 6 ^{3}P$_1$ resonance.

Curves (f)–(h) in Figure 5 were recorded with λ_1 tuned to the high energy (blue) side of the 6 ^{3}P$_1$ resonance. Note that these curves have been multiplied by factors of 8, 8, and 4, respectively, indicating significantly lower conversion efficiencies in this region. The relatively low intensities for curves (f) and (g) are attributable to the fact that χ_1 approaches zero just to the blue of the resonance, as shown in Fig. 4. The increased conversion efficiency observed for curve (h), with λ_1 tuned further from the atomic resonance, is due to the larger χ_1 and χ_{VUV} in this region.

As illustrated in Figure 5 (curves (a)–(e)), the VUV tuning curves become narrower as the VUV energy approaches the 9P resonance from the low-energy side. This behavior can be understood from the calculations of Smith and Alford.[20] As illustrated in Figure 3, the slope of the plot of the index mismatch Δk vs. photon energy increases as atomic resonances are approached. The choice of input wavelength λ_1 in the vicinity of the ^{3}P$_1$ resonance at 253 nm dictates VUV wavelength where maximum conversion efficiency can be achieved. The VUV tunability (i.e., tunability of λ_3) is limited by the requirement that the partial index mismatch Δk falls within a range specified by λ_1. At VUV wavelengths far away from the 9P resonance where Δk varies weakly with λ_3, a relatively wide range of VUV wavelengths fall within the specified Δk. However, near resonances, the much stronger dependence of Δk on λ_3 (steeper slope in Fig. 3), leads to a narrower range of VUV tunability.

B. Absolute VUV pulse energy measurements

In order to determine the absolute VUV pulse energies, we have compared signals from the non-reactive scattering of n-methylaniline from O_2 using the 7.9 eV output of an F_2 excimer laser and our 9.9 eV light source. We found that the total signal level using the 9.9 eV light source using the 266.1 nm + 379.5 nm mixing scheme (curve (a) in Figure 5) is 6 times smaller than that of the 7.9 eV light source. We have measured the 7.9 eV pulse energy using a pyroelectric energy meter to be 1.0 mJ/pulse ($\sim 8 \times 10^{14}$ photons/pulse). Using the 8×10^{14} photons/pulse value at 7.9 eV and correcting for the factor of 3 difference in photoionization cross section of n-methylaniline between 7.9 eV and 9.9 eV;[30] we conclude that 0.07 mJ/pulse at 125 nm is delivered to the ionization region of the detector at the peak of curve (a) in Figure 5. Assuming 70% transmission through the MgF_2 lens, this corresponds to 0.10 mJ/pulse at 125 nm, i.e., 6×10^{13} photons/pulse. At 30 Hz, this corresponds to 1.8×10^{15} photons/s.

Our measured VUV pulse energy at 125 nm is a factor of $\sim$10 smaller than that reported previously near 130 nm using three transform-limited pulsed lasers, each providing $\sim$10 mJ/pulse.[21] The principal differences between our conditions and those reported earlier are that our lasers are multimode with bandwidths of $\sim$0.15 cm^{-1} each ($\sim$0.21 cm^{-1} after frequency doubling) rather than Fourier transform limited. Also, the spatial quality of the beams produced by commercial dye lasers deviate significantly from the Gaussian distributions employed in the previous work. In our experiment, the 255 nm pulse energy was limited to 2.7 mJ because only a single Nd:YAG laser was available for pumping all three dye lasers. Also, our pulse duration was substantially longer ($\tau \sim 7.0$ ns) than that in the previous experiments ($\sim$2.2 ns). Using these parameters, the calculated peak 255 nm laser power in our work (0.43 MW) is about an order of magnitude smaller than in the work of Muller (4.5 MW).[21]

C. VUV generation near the 130.2 nm $^3P_J \rightarrow {}^3S_1$ transition in atomic oxygen

We have demonstrated the tunability of the high-intensity light source by tuning to the atomic oxygen $^3P_2 \rightarrow {}^3S_1$ transition at 130.2 nm.[26] In these studies, a photon at 130.2 nm photodissociates O_2 molecules and then a second 130.2 nm photon (within the same laser pulse) excites the oxygen atoms to the $^3S_1$ state. A 305 nm photon from another dye laser then promotes the oxygen atoms to high-n Rydberg levels. The atoms drift to a microchannel plate where they are field ionized and counted as a function of arrival time and laboratory angle.[26]

Several different studies of molecular photoionization in our laboratory indicate that the VUV pulse energies produced near 130 nm are very similar to those obtained at 125 nm. On the basis of calculated χ values,[20] this is anticipated. Typical time-of-flight spectra for $O(^3P_2)$ products are shown in Figure 6. The peak at shorter arrival time corresponds to $O(^3P_2)$ recoiling from $O(^3P_{0,1,2})$ and the peak at later time corresponds to $O(^3P_2)$ recoiling from $O(^1D_2)$. The absolute signal levels using VUV pulses generated in Hg vapor are greater by more than two orders of magnitude compared to that obtained previously under otherwise similar conditions using the 2-1 mixing scheme in Kr employing tunable lasers at 212.55 and 580 nm.[26,31,32] Since the observed signals result from absorption of two 130 nm photons, and either or both of the transitions may be saturated using the high intensity VUV source, it is difficult to make quantitative statements about the relative intensities based on these measurements. However, in recent studies of the metastable $O(^1S_0)$ product signal from N_2O photodissociation at 130 nm, involving a single photon process, we observe signals that are a factor of ~300 times greater than using the previous method.[31] This is consistent with the expectation that our previous pulses were $\sim 1 \times 10^{11}$ photons/pulse for resonant (but not phase matched) 2-1 mixing in Kr[3,15] and our conclusions that the 130 nm intensities are comparable to those produced near 125 nm, measured to be 3×10^{13} photons/pulse. The large increase in 130.2 nm laser intensities, combined with the much smaller background levels resulting from removing the UV and visible laser beams opens up the possibility to study a range of chemical reactions producing ground state oxygen atoms in crossed molecular beams, such as $H + O_2 \rightarrow OH + O$.

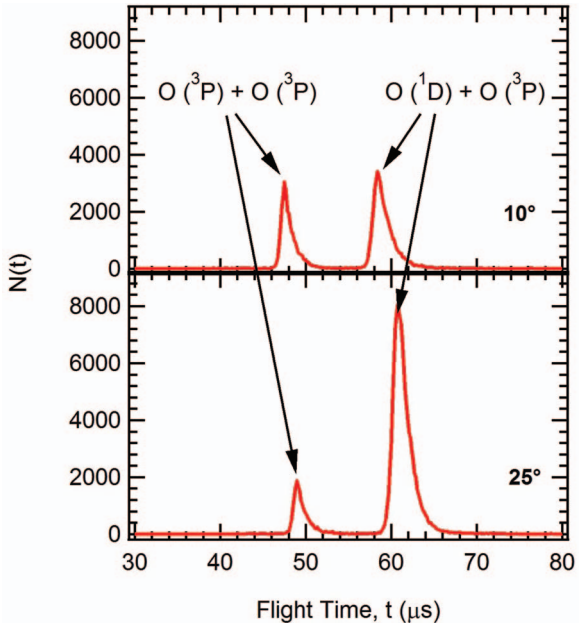

FIG. 6. Time-of-flight spectra for $O(^3P_2)$ atoms produced by O_2 photodissociation at 130.2 nm monitored by ORTOF. Laboratory angles are indicated.

We have not recorded VUV tuning curves in the 130 nm range similar to those shown in Fig. 5 near 125 nm. However, we have scanned ν_3 at various combinations of ν_1 and ν_2 in order to map out optimum phase matching curves and efficiencies. The behavior observed in these studies was very similar to that observed near 125 nm. Most notably, we found that the highest VUV intensities were always observed on the red side of the $^3P_1$ resonance, and VUV intensities did not change significantly within 200 cm^{-1} of the $^3P_1$ resonance.

D. Prospects for increased VUV pulse energies

As shown in Fig. 5, the greatest VUV intensities (0.10 mJ/pulse) were obtained using three tunable dye lasers with ν_1 tuned to the low energy side of the 6 $^3P_1$ resonance. An input pulse energy of 2.7 mJ at 255 nm corresponds to 3.5×10^{15} photons/pulse. Using our measured VUV intensity of 6×10^{13} photons/pulse at 125 nm corresponds to a 1.7% conversion efficiency from the UV to VUV. This is a factor of about 3 smaller than the 5% conversion efficiency reported by Muller and co-workers using three pulse amplified ring dye lasers, which produced 1.1 mJ VUV pulses at 130 nm.[21] Note that our final pulse energies (0.1 mJ) are about a factor of ten smaller.

Laser power dependence measurements in our laboratory revealed that the VUV intensities increase approximately linearly with 255 nm pulse energies up to 2.7 mJ, with no evidence for the onset of saturation in the conversion efficiency with increasing ν_1 pulse energies. On the other hand, using 2.7 mJ pulses at 255 nm, further increases in pulse energies at 404 nm and 625 nm produce increases in VUV intensities that are much less than linear, suggesting the onset of saturation in conversion efficiencies for ν_2 and ν_3 under our experimental configuration. In the work of Muller, 255 nm pulse energies were 10 mJ, with pulse durations of 2.2 ns.[21] Since our pulse intensities were a factor of 3 smaller, and pulse duration (~7 ns) a factor of three greater, it is tempting to attribute the order of magnitude smaller VUV intensities produced in our work to the order of magnitude smaller 255 nm laser powers we employed.

On the basis of our measurements, the most obvious way to further increase our VUV pulse energies is by increasing the 255 nm pulse energy. In our experiments to date, the 255 nm pulse energies were limited to 2.7 mJ by the available Nd:YAG pump energy and relatively low efficiency for third harmonic generation starting with a 765 nm dye laser. We attempted to obtain higher 255 nm pulse energies by frequency doubling the 510 nm radiation from a 355 nm pumped dye laser, or by mixing the 532 nm from the Nd:YAG laser with

480 nm produced by a 355 nm pumped dye laser. However, in both cases the maximum pulse energies were still ∼3 mJ. However, by employing a second Nd:YAG laser for pumping the three dye lasers, and/or by employing a different nonlinear mixing scheme for production of 255 nm light (e.g., doubling of 666 nm light to 333 nm followed by mixing with 1064 nm), achieving 255 nm pulse energies of ∼10 mJ should be feasible. We note that by employing a second Nd:YAG pump laser, higher pulse energies at 404 nm and 625 nm (or 777 nm) can also be obtained. Thus, on the basis of our power dependence measurements, by employing 255 nm pulse energies in the 10 mJ range, at least a threefold increase in VUV pulse energies, i.e.,∼0.3 mJ/pulse should be readily achievable.

Detailed modeling of the four-wave mixing process to generate 130.2 nm radiation has been carried out, with the primary aim being to maximize conversion efficiencies.[33,34] A number of considerations were presented in these papers that, if implemented, may lead to substantial improvements to the efficiencies reported here. To date, however, we have not employed these concepts to improve conversion efficiencies. We have also not yet attempted to improve the laser beam spatial profiles by spatial filtering of the dye laser beams prior to amplification. Also, the beam diameters of the three laser beams were set to be nominally equal by employing the same telescope configurations in each laser prior to final amplification. We have not attempted to quantitatively match (using a laser beam profiler) the spatial beam diameters of the three input beams prior to mixing. We have not devoted any effort to optimizing conversion efficiencies by simultaneously varying the diameters of the three input laser beams. Also, in the original work of Muller and co-workers, considerable effort was devoted to ensuring that the heat pipe temperature was uniform throughout using a secondary enclosure. As noted in Sec. II, other than wrapping the heat pipe with copper foil, we have not taken great care to ensure homogeneous temperature. Clearly, many experimental parameters are subject to substantial further optimization, leading to further increases in VUV pulse energies. From these considerations, we believe that with some care, pulse energies in the 1 mJ range near 125 nm or 130 nm are within reach using commercial nanosecond dye lasers.

E. Generation of VUV at 120 nm < λ < 125 nm

The calculations by Smith and Alford cover VUV energies up to 83 100 cm^{-1}, i.e., down to $\lambda \approx 120$ nm.[20] Behavior similar to that shown in Figures 3 and 4 was observed. The VUV conversion efficiencies are expected to decrease at shorter wavelengths due to the smaller χ_{VUV}. While this range includes Lyman-α at 82 259 cm^{-1}, χ_{VUV} is very small for Hg at this specific wavelength, so conversion efficiencies will be substantially smaller than those reported in this paper. Consequently, resonance enhanced difference frequency mixing in Kr/Ar mixtures ($\nu_{VUV} = 2\nu_1 - \nu_2$) is likely to remain the best approach for VUV generation at Lyman-α.[3] We note, however, that using $\lambda_1 = \lambda_2 = 312.85$ nm and $\lambda_3 = 581$ nm indicates that the peak VUV intensities near 123 nm are similar to those near 125 nm.

F. Generation of VUV at λ < 120 nm

Because of the reduced transmission of the MgF_2 output window at shorter wavelengths, we have not carried out extensive studies at $\lambda < 120$ nm using collimated input laser beams in Hg. However, during the course of this work, we found that substantial VUV intensities are generated near 11.0 eV ($\lambda \approx 112.7$ nm) using only two lasers with $\lambda_1 = 255$ nm, $\lambda_2 = 404$ nm, and $\lambda_3 = 404$ nm, corresponding to VUV energies well above the Hg^+ limit at 84 184 cm^{-1}. Relatively strong photoionization signals were observed, despite the fact that the transmission through our MgF_2 lens must be very small (<10%). Since an excited state of Hg lies at 88 759 cm^{-1}, it is perhaps not surprising that VUV generation is efficient near 11.0 eV. Using an off-axis MgF_2 lens configuration, the 112.7 nm light is spatially dispersed from the 125 or 130.2 nm beams, and would normally not contribute. It is important to keep in mind, however, that with $\lambda_1 = 255$ nm and $\lambda_2 = 404$ nm (e.g., for producing light at 130.2 or 125 nm), in the absence of a dispersing element, significant VUV light at 112.7 nm is likely to be present, especially if a LiF optic is used as the VUV exit window.

It is well-known that Hg facilitates efficient production of radiation at wavelengths well below the LiF cutoff at 104 nm.[35,36] The most challenging aspects of generation of light in the XUV is designing a cell facilitating windowless operation, and developing a method for spatially isolating the XUV without energy losses inherent to dispersive elements such as gratings. We have recently been working on the generation of light at energies up to 13 eV, and have made considerable progress in both of these areas.[37]

V. CONCLUSIONS

Generation of intense pulsed VUV radiation (6×10^{13} photons/pulse) has been demonstrated using resonance-enhanced four-wave mixing of unfocussed pulsed commercial dye lasers in Hg vapor. The tuning curves for a number of different resonant two-photon combinations have been measured and agree well with the predictions of Smith and Alford.[20] While the highest conversion efficiencies (1.7% from UV to VUV) and peak intensities are achieved using three independently tunable dye lasers, two somewhat simpler schemes employing two dye lasers are characterized. Our studies indicate that under our experimental conditions, VUV pulse energies are limited by the available input pulse energies at 255 nm and that further increases in VUV pulse energies to the mJ range should be readily achievable.

ACKNOWLEDGMENTS

This research was supported by the National Science Foundation under Grant No. CHE-0809622 (Transition Metal Chemistry) and by the Office of Science, U.S. Department of Energy, under Grant No. DE-FG02-00ER15095 (Free Radical Chemistry). The authors wish to acknowledge Dr. Arlee V. Smith (AS-Photonics, Albuquerque, NM) for permission to reproduce data in Figures 3 and 4 and for valuable discussions.

[1]D. N. Nikogosyan, *Nonlinear Optical Crystals: A Complete Survey* (Springer Science Inc., New York, 2005).
[2]R. Hilbig and R. Wallenstein, Appl. Opt. **21**, 913 (1982).
[3]J. P. Marangos, N. Shen, H. Ma, M. H. R. Hutchinson, and J. P. Connerade, J. Opt. Soc. Am. B **7**, 1254 (1990).
[4]E. Cromwell, T. Trickl, Y. T. Lee, and A. H. Kung, Rev. Sci. Instrum. **60**, 2888 (1989).
[5]S. J. Hanna, P. Campuzano-Jost, E. A. Simpson, D. B. Robb, I. Burak, M. W. Blades, J. W. Hepburn, and A. K. Bertram, Int. J. Mass Spectrom **279**, 134 (2009).
[6]S. Souma, T. Sato, T. Takahashi, and P. Baltzer, Rev. Sci. Instrum. **78**, 123104 (2007).
[7]F. Mühlberger, J. Wieser, A. Morozov, A. Ulrich, and R. Zimmermann, Anal. Chem. **77**, 2218 (2005).
[8]R. Flesch, M. C. Schürmann, M. Hunnekuhl, H. Meiss, J. Plenge, and E. Rühl, Rev. Sci. Instrum. **71**, 1319 (2000).
[9]X. Yang, J. Lin, Y. T. Lee, D. A. Blank, A. G. Suits, and A. M. Wodtke, Rev. Sci. Instrum. **68**, 3317 (1997).
[10]S.-H. Lee, C.-H. Chin, W.-K. Chen, W.-J. Huang, and C.-C. Hsieh, Phys. Chem. Chem. Phys. **13**, 8515 (2011).
[11]G. C. Bjorklund, IEEE J. Quantum Electron. **11**, 287 (1975).
[12]R. Mahon, T. J. McIlrath, V. P. Myerscough, and D. W. Koopman, IEEE J. Quantum Electron. **15**, 444 (1979).
[13]H. Langer, H. Puell, and H. Röhr, Opt. Commun. **34**, 137 (1980).
[14]R. Hilbig and R. Wallenstein, IEEE J. Quantum Electron. **17**, 1566 (1981).
[15]G. Hilber, A. Lago, and R. Wallenstein, J. Opt. Soc. Am. B **4**, 1753 (1987).
[16]B. R. Strazisar, C. Lin, and H. F. Davis, Science **290**, 958 (2000).
[17]L. Hanley and R. Zimmermann, Anal. Chem. **81**, 4174 (2009).
[18]R. Mahon and F. S. Tomkins, IEEE J. Quantum Electron. **18**, 913 (1982).
[19]R. Hilbig and R. Wallenstein, IEEE J. Quantum Electron. **19**, 1759 (1983).
[20]A. V. Smith and W. J. Alford, J. Opt. Soc. Am. B **4**, 1765 (1987).
[21]C. H. Muller, D. D. Lowenthal, M. A. DeFaccio, and A. V. Smith, Opt. Lett. **13**, 651 (1988).
[22]R. G. Caro, A. Costela, and C. E. Webb, Opt. Lett. **6**, 464 (1981).
[23]K. S. E. Eikema, J. Walz, and T. W. Hänsch, Phys. Rev. Lett. **83**, 3828 (1999).
[24]D. Kolbe, M. Scheid, and J. Walz, Phys. Rev. Lett. **109**, 063901 (2012).
[25]D. R. Albert and H. F. Davis, J. Phys. Chem. Lett. **1**, 1107 (2010).
[26]C. Lin, M. F. Witinski, and H. F. Davis, J. Chem. Phys. **119**, 251 (2003).
[27]P. A. Willis, H. U. Stauffer, R. Z. Hinrichs, and H. F. Davis, Rev. Sci. Instrum. **70**, 2606 (1999).
[28]D. Proch and T. Trickl, Rev. Sci. Instrum. **60**, 713 (1989).
[29]D. L. Proctor, D. R. Albert, and H. F. Davis, Rev. Sci. Instrum. **81**, 023106 (2010).
[30]M. Xie, Z. Zhou, Z. Wang, D. Chen, and F. Qi, Int. J. Mass Spectrom **303**, 137 (2011).
[31]M. F. Witinski, M. Ortiz-Suárez, and H. F. Davis, J. Chem. Phys. **122**, 174303 (2005).
[32]M. F. Witinski, M. Ortiz-Suárez, and H. F. Davis, J. Chem. Phys. **124**, 094307 (2006).
[33]A. V. Smith, W. J. Alford, and G. R. Hadley, J. Opt. Soc. Am. B **5**, 1503 (1988).
[34]A. V. Smith, G. R. Hadley, P. Esherick, and W. J. Alford, Opt. Lett. **12**, 708 (1987).
[35]C. H. Kwon, H. L. Kim, and M. S. Kim, Rev. Sci. Instrum. **74**, 2939 (2003).
[36]P. R. Herman and B. P. Stoicheff, Opt. Lett. **10**, 502 (1985).
[37]M. A. Todd, D. R. Albert, and H. F. Davis, "High-intensity VUV and XUV Generation by Noncollinear Four-wave Mixing in Laser Vaporized Media" (unpublished).